Ind. J. Pharm. Edu. Res., 2026; 60(1s):s83-s92.
https://www.ijper.org

Original Article

Formulation and Characterization of Clotrimazole Loaded Polymeric Nanoparticles Fabricated by Single Emulsion Evaporation Technique

Valikala Viswanath[1,*], Palla Venkata Murali Krishna[2], Vankam Lokeswara Babu[3], Tanuja Anajigere Mruthunjaya Lakkamma[3]

[1]Department of Pharmaceutics, Annamacharya College of Pharmacy, Rajampeta, Annamaiah, Andhra Pradesh, INDIA.
[2]Department of Pharmaceutical Analysis, KLE College of Pharmacy, Bengaluru, Karnataka, INDIA.
[3]Department of Pharmaceutics, Danigond College of Pharmacy, Terdal, Bagalkote, Karnataka, INDIA.

ABSTRACT

Aim/background: Utilizing nanotechnology allows us to shrink machinery down to the atomic level, leading to groundbreaking progress in technical innovation. Our most recent efforts concentrated on developing polymeric nanoparticles loaded with clotrimazole to investigate their antifungal abilities. **Materials and Methods:** Polymeric nanoparticles were synthesized by blending aqueous polyvinyl alcohol with methanolic polycaprolactone and clotrimazole in various ratios. The mixture underwent high-speed homogenization, ultrasonication, and magnetic stirring to facilitate the formation and recovery of the nanoparticles. **Results:** FTIR analysis confirmed the presence of essential functional groups and ruled out drug-excipient incompatibilities. Particle size measurements ranged from 80.24±0.03 to 142.18±0.06 nm, with a zeta potential between -21.9 mV and -13.2 mV. SEM and TEM images revealed that particles were uniformly sized below 50 nm, though occasional aggregation was observed. AFM and XRD studies revealed the crystalline nature of nanoparticles with an average diameter of 25±10 nm and a height of 40±15 nm. The antifungal investigations demonstrated substantial antifungal efficacy against resistant *C. glabrata* and *C. albicans* strains, with MIC values of 25.3±0.4 and 23.2±0.3, and IC_{50} values of 273.3±2.8 and 362.2±0.4, respectively. **Conclusion:** The study developed clotrimazole-loaded polymeric nanoparticles with optimized size, shape and zeta potential for effective membrane penetration and stability. Comprehensive spectroscopic, microscopic, and thermal analyses confirmed that the nanoparticles were spherical, pure, and crystalline with strong antifungal activity against resistant *C. glabrata* and *C. albicans*, suggesting promising potential potential for future commercial use.

Keywords: Nanoparticles, Nanosystems, Nanocarriers, Nanomaterials, Nanostrutures and Clotrimazole.

Correspondence:
Dr. Valikala Viswanath
Professor, Department of Pharmaceutics, Annamacharya College of Pharmacy, Rajampeta, Annamaiah-516126, Andhra Pradesh, INDIA.
Email: viswanath.prrm@gmail.com

Received: 02-05-2025;
Revised: 19-06-2025;
Accepted: 28-08-2025.

INTRODUCTION

The complexity associated with diseases and their treatment pose novel challenges to the pharmaceutical drug delivery systems to selectively target the drug entities and elicit the pharmacological response. The therapeutic effectiveness relies on fundamental parameters such as particle diameter and its surface interaction with the targeted cellular membranes that results in the effective drug uptake. The internalization of the nanocomposites rely on numerous factors such as particle shape, diameter, zeta potential, surface characteristics, and the interacting cell etc.,[1,2]

The structural composition of nanoparticles comprises three components namely, hydrophobic core region, hydrophilic polymeric shell, and a lipid monolayer at the interface between the shell and core region. The nanoparticles offer various advantages such as enhanced bioavailability, efficacy, drug delivery and drug targeting characteristics with reduced toxicity with superior biological stability, decreased enzymatic degradation and high encapsulation efficacy for various drug molecules. The nanoparticles are encapsulated with various biocompatible and biodegradable polymers which enable them to reveal exciting drug delivery characteristics such as sustained release, controlled release, tissue targeting, and carrier mediated transport for various proteins, peptides, and oligonucleotides.[3] Therefore the current exploration defines the pharmaceutical nanoparticles as colloidal particles of submicron size loaded with suitable drug molecules. The term nanoparticle is collectively designed for both nanocapsules and nanospheres. The nanocapsules are

DOI: 10.5530/ijper.20260603

categorized under vascular drug delivery systems in which the drug is localized at the liquid core region encapsulated with a polymer. The drug molecules can be localized either at the core region or adsorbed at the terminal region to modify their release attributes. In contrary, the nanospheres belong to matrix-type where the drug molecules are either encapsulated at the interior region or terminally anchored to enhance their permeability and localization characteristics.[4] The optimization of experimental variables generates the nanoparticles with optimized size devoid of toxic residues. The experimental methodology for the production of nanoparticles should be refined because it influences the physiochemical properties of the dosage form. The current exploration prefers solvent evaporation technique which is widely preferred for the fabrication of nanoparticles. The technique offers flexibility for the encapsulation of miscellaneous drug molecules with varied release characteristics. The technique has undergone several modifications and well-established to encapsulate various hydrophilic and lipophilic molecules. The morphological attributes of drug carriers are influenced by degree of homogenization, qualitative and quantitative ratio of excipients, and surfactant characteristics.[5,6] Clotrimazole is an imidazole derivative classified under antifungal agents and referred for the treatment of miscellaneous infections. The Clotrimazole is not favored for oral route of administration because it elicits potent side effects with decreased half-life and demands frequent dosing to maintain the steady state concentrations. Furthermore, Clotrimazole has low aqueous solubility and demand an appropriate dosage form that fulfills the pharmacokinetic and pharmacodynamic requirements. The Clotrimazole exerts the antimycotic action via ergosterol inhibition and alteration of cell membrane potential that results in the leakage of internal components and cell lysis.[7] Therefore, we fabricated the polymeric nanoparticles of Clotrimazole to report the drug delivery and antifungal characteristics.

MATERIALS AND METHODS

The clotrimazole and polycaprolactone were dissolved in methanol and added drop by drop to the polyvinyl alcohol aqueous solution (i.e. definite amount of polyvinyl alcohol in 100 mL of water) with high speed homogenization for 15 min of 3 cycles and 40 sec time interval. The mixture is subject for ultrasonification using a probe sonicator for a couple of minutes. The resultant emulsion was subjected to magnetic stirring at 1000 rpm for 5 to 6 hr for complete evaporation of the organic solvent. The resultant nanoparticles were recovered by centrifugation at 18,000 rpm for 30 min and washed with distilled water for thrice to remove the surfactant. After the purification, the nanoparticles were freeze dried to obtain them in fine powdered form and placed in a vacuum desiccator. The detailed formulation chart for the preparation of nanoparticles comprising varied concentrations of the critical ingredients is listed in Table 1 for reference.[8-10]

Evaluation of nanoparticles

Attenuated Total Reflectance Spectroscopy (ATR)

The ATR technique allows the evaluation of drug excipient incompatibilities via direct examination of liquid or solid samples without further preparation. The technology utilizes total internal reflection to produce an evanescent wave that penetrates through the sample and furnishes the critical molecular information. The nanoparticles and critical excipients used in the formulation are subjected to ATR analysis to generate a characteristic spectrum whose characteristic peak interpretation for various functional groups enables to enumerate the possible incompatibilities.[11-13]

Particle size and Zeta potential

The Particle size and Zeta potential are determined to predict the particle size and terminal charge of the nanoparticles. The particle size and terminal charge is determined by using dynamic light scattering technique using a Zeta Sizer Naano-ZS. The instrumentation was fitted with laser emission at 633 nm and backscattering at an angle of 173° and the samples were suitably diluted in deionized water and measured at 25°C. In a similar fashion, the zeta potential of the nanoparticles is estimated at 25°C using the Marven Zeta Sizer Naano-ZS and the results are recorded.[14-17]

Drug Content and entrapment efficacy studies

Accurately weighed nanoparticles were dissolved in methanol and kept aside. To the resultant, 100 mL of phosphate buffer solution (pH 7.4) is added and subjected to magnetic stirring for evaporation of organic solvent and complete extraction of clotrimazole. The polycaprolactone which is precipitated is removed by filtration and the amount of drug in the filtrate is determined spectrophotometrically at 260 nm.[18-20] The entrapment efficacy and the drug content are determined by using the following equations:

$$\text{Entrapment efficacy(EE\%)} = \frac{\text{Mass of drug in the nanoparticles}}{\text{Massof drug in the formulations}} \times 100$$

$$\text{Drug Content (\% w/w)} = \frac{\text{Mass ofdrug in nanoparticles}}{\text{Mass of nanoparticles recovered}} \times 100$$

In vitro drug release studies

The *in vitro* drug releases were determined by using dialysis bag diffusion technique. The nanoparticles were dispersed in the methanolic PBS pH 6.4 (30%v/v of methanol) and kept aside. The egg permeability membrane is used for dialysis in which one end of the hollow test tube is attached to egg permeability membrane and used a sac for dialysis. The predefined quantities of the nanoparticles are placed in the sac which is used as the donor compartment and the methanolic buffer solution acts as the receiver compartment. The donor compartment is immersed in the receiver compartment and rotated at 100 rpm at 37±0.5°C. The drug released from the nanoparticles goes inside the receiver compartment from which aliquots of the sample is withdrawn

intermittently at predefined time intervals, diluted and analyzed spectrophotometrically at 260 nm to estimate the drug release.[21-23]

Kinetic parameters

The dissolution profile of individual formulations is fitted into various kinetic equations to enumerate the drug release mechanism from the dosage form. The equation $Q_{t=}K_0t$ represents zero order kinetics, In $Q_{t=}$In Q_0-K_1t represents first order, $Q_{t=}K_h\ t^{1/2}$ signifies Higuchi model, and $M_t/M_\alpha=K_pt^n$ for Korsemeyer-Peppas model respectively. In the above equations Q_t indicate the drug release in time t, Q_0 indicate the initial drug concentration in the nanoparticles, and K_0, K_1, K_h, and K_p are the constants. After fitting the statistical data into various kinetic models, the regression coefficient (R^2) values are determined from the slope of the equations and for Korsemeyer-Peppas model the release exponent "n" is determined to explore the drug release mechanism. If the exponential value "n" is 0.45, the drug release follows Fickian mechanism, and if the values range from 0.45<n< 0.89, it follows non-fickain (anomalous) mechanism, if n=0.89, it follows case II transport and if n>0.89, it follows super case II transport.[24,25]

Microscopic studies

Scanning Electron Microscopy (SEM)

Scanning electron microscopy is a potent analytical technique used for the characterization of nanomaterials. The SEM studies are carried out using JEOL, JSM -67001 in which an electron beam is used to scan the samples and the electron-sample interactions produce high resolution images that explore the morphological characteristics and chemical composition of the nanoparticles.[26-28]

Transmission Electron Microscopy (TEM) Studies

The TEM studies are performed by using JEOl-JEM-1200EX microscope functioning at 100kV and equipped with AMT XR41-B 4-megapixel (2048) bottom mount CCD camera to obtain the high resolution images at various magnifications. The images generated were measured with the aid of Image J software ver. 1.49h and the morphological characteristics were predicted accordingly. In brief, a 15 µL of nanoparticle suspension was deposited on carbon-layered copper grids and gently dried using a Whatmann filter paper. After 30 min, the resultant was stained with a drop of phototungstic acid and the examined under the microscope to explore the morphological characteristics of the nanoparticles.[29-31]

X-ray Diffraction studies (XRD)

The X-ray diffraction is a potent analytical technique used for exploring the crystalline phases of nano materials and to detail the structural characteristics. The XRD studies are characterized at a diffraction angle ranged from 10° to 80° with 0.02° steps and operated at 30 mA and 40 kV at a wavelength of 1.54 Å using Rigaku D-max 2400 diffractometer. The x-ray diffractometer is exclusively used for the characterization of physiochemical properties of drug molecules such as phase composition, crystal structure and its orientation in liquid, solid and powdered samples. In X-ray diffraction, various crystalline phases exhibit various diffraction patterns, which can be compared with the existing standard patterns in the reference databases such as International Center of Diffraction Data (ICCD) and the conclusions are drawn out. A linear correction was applied to the observed peak before deriving the area under the corresponding peak.[32-34] The following formula is used to determine the degree of crystallinity and to calculate the areas corresponding to the crystalline and amorphous phases in arbitrary units.

$$X_c = \frac{I_c}{I_a + I_c}$$

Where, I_a and I_c represents the integrated intensities corresponding to amorphous and crystalline phases respectively.

Atomic Force Microcopy (AFM)

To ensure optimal sample preparation for atomic force microscopy, the sample is carefully diluted with deionized water to achieve a concentration of 1 mg/mL. Following this, a precise 20 µL suspension is applied to mica, hydrophobic, and hydrophilic silicon surfaces, and then dried at 37±0.5°C overnight for impeccable results. The AFM was meticulously developed using the Park Systems XE-100 AFM in contact mode. The silicon nitride probes are equipped with cantilevers measuring 196 nm in length and boasting a 0.12 N/m spring constant with forces applied between 3 and 10 nm and a 10 nm radius of curvature. The scan was optimized to run at a speed between 1 and 3Hz, and the resulting parameters were presented as average±standard deviation for almost 50 samples.[35-37]

Anti-fungal studies

Microorganism and their test medium

C. glabrata (MTCC-184) and *C. albincans* (MTCC-183) were preferred for investigating the antifungal activity of the nanoparticles. The dextrose agar media was used for the inoculation of strains incubated at 35±0.5°C for 24 hr followed by sub culturing at 35±0.5°C for 24 hr=The sample solution was prepared by diluting with normal saline i.e. 0.9% NaCl to produce $1x10^9$ CFU/mL. The sample was diluted with RPMI-1640 medium (comprising L-glutamine excluding sodium bicarbonate) comprising 0.2M 3-(N-Morpholino) Propanesulfonic acid (MOPS) to generate the final concentration to $0.5x10^6$ CFU/mL.

Minimum Inhibitory Concentration (MIC) and Inhibitory Concentration 50% (IC_{50})

C. glabrata (MTCC-184) and *C. albincans* (MTCC-183) were preferred for the investigating the antifungal attributes of the polymeric nanoparticles. The strains were incorporated into a sterile 96 well microtiter plate followed by addition of 100 µL

of Clotrimazole (2-80 µg/mL) and 200 µL of deionized water to inhibit the rapid evaporation of the culture medium during incubation. The suspensions comprising individual stains (absence of Clotrimazole) and comprising media (as background control) were added to two wells and its optical density was determined at 35±0.5°C at 405 nm for 24 hr. The growth curves were analyzed and the difference in the turbidometry reflected the optical density with respect to individual drug concentrations. The MIC and IC_{50} were determined statistically and reported after eliminating the optical density in their background. The kinetic curves were plotted to estimate the IC_{50} values whose slopes represented the potentiality of Clotrimazole against fungal infections.[38-41] The percentage growth against the Clotrimazole concentrations is represented by the following equation:

$$\text{Growth \%} = \frac{\text{OD of wells comprising Clotrimazole}}{\text{Optical density of wells devoid of Clotrimazole}} \times 100$$

RESULTS AND DISCUSSION

ATR Studies

The drug excipient incompatibility studies are determined using ATR studies. The native clotrimazole structure reveals the presence of C=C stretch (1600-1500 cm^{-1}) which is identified at 1583.95 cm^{-1} in the clotrimazole substance and the same at 1580.00 cm^{-1} in the nanoparticles. The presence of C-C stretch, C-H stretch, and C-H bending are identified at 1565.17 cm^{-1}, 3062.43 cm^{-1}, 1433.29 cm^{-1} for clotrimazole while they are pointed at 1560.00 cm^{-1}, 3014.48 cm^{-1}, and 1436.52 cm^{-1} in nanoparticles respectively, In addition, the characteristic peaks for C=N and C-Cl stretch are reveled at 1650.76 cm^{-1} and 706.95 cm^{-1} for clotrimazole while the corresponding functionalities are specified at 1650.53 cm^{-1} and 701.46 cm^{-1} in the nanoparticles respectively. The spectral characterization of polycaprolactone revels the presence of CH_2 asymmetric stretch at 2936.87 cm^{-1}, C=O stretch at 1706.24 cm^{-1}, an intense O-H stretch at 3273.58 cm^{-1}, and C-H stretch for secondary alcohol at 1081.18 cm^{-1}. In addition, the spectral characterization of polyvinylalcohol reveals the presence of C-H stretch at 2905.36 cm^{-1}, C=O stretch at 1705.24 cm^{-1}, C-O stretch at 1235.55 cm^{-1}, C-C stretch at 1416.54 cm^{-1} respectively (Figure 1). The spectral characterization of the polymeric nanoparticles does not specify any supplementary peaks which represents the absence of pharmaceutical incompatibilities and assures the stability of nanoparticles.

Drug content

The drug loading is influenced by the critical parameters such as polymer molecular weight, potential functional groups, solubility of the drug, and interactions between the drug and the polymer. An increase in the drug loading increased the particle size and zeta potential of the nano particles. The experimental results reveal maximum drug content of 93.27±0.05% for CTF4 and least for CTF8 with 90.02±0.03% (Table 2). The theoretical interventions reveal a proportionate increase in the drug content with particle size, but the experimental results reflect a slight variation in the drug content between the formulations which might be due to the methodology adopted and the difference in the concentration of polycaprolactone and polyvinylapcohol. Furthermore, the drug content determination involves extraction of clotrimazole from the nanoparticles followed by filtration which is a tedious process and initiated the drug loss.

Entrapment Efficacy (%)

The experimental results revealed that an increase in the polycaprolactone (polymer) concentrations and optimized methanol (organic solvent) concentration has increased the entrapment efficacy while a decrease in the polyvinyl alcohol (surfactant) concentration has increased the entrapment efficacy. The theoretical background for the proportionate increase in the entrapment efficacy might be due to enhanced viscosity of the organic phase which enhanced the resistance for drug molecules to penetrate from organic to aqueous phase and entrapped them in the nanoparticles. In the current investigation, the concentration of methanol was optimized to 5 mL to maintain an optimized viscosity of the nano formulations. The entrapment efficacy for various formulations ranged from 67±0.08 to 85±0.02% respectively. The investigative findings revealed that the entrapment efficacy increased proportionally from CTF1 to CTF4 and ranged from 67±0.08 to 85±0.02%.

Table 1: Formulation details of Clotrimazole nanoparticles.

Formulation	Clotrimazole (mg)	Polycaprolactone (mg)	Polyvinyl alcohol (% w/v)	Methanol (mL)	Water (mL)
CTF1	0.25	100	0.065	5	20
CTF2	0.25	200	0.070	5	20
CTF3	0.25	300	0.075	5	20
CTF4	0.25	400	0.080	5	20
CTF5	0.25	500	0.085	5	20
CTF6	0.25	600	0.090	5	20
CTF7	0.25	700	0.095	5	20
CTF8	0.25	800	0.100	5	20

Further, an increase in the concentrations of polycaprolactone and poly vinyl alcohol, the entrapment efficacy decreased erroneously and ranged from 69±0.02% to 81±0.03% (Table 2) because it encouraged the rapid penetration of drug molecules into the aqueous phase during emulsification and decreased the availability of drug molecules in the emulsion droplets for effective interaction with polycaprolactone. However, the organic phase when diffused from the oil phase to the external aqueous phase allowed the particles to harden. In contrary, CTF1 comprises low concentrations of polycaprolactone and polyvinyl alcohol that led to high polydispersity and particle aggregation whereas; CTF8 consists of elevated polycaprolactone and polyvinyl alcohol concentrations that encouraged the interaction between the drug and surfactant which decreased the drug loading. Hence, an optimized concentration of surfactant is recommended for the effective nanoparticle formulation. In addition, the decline in the entrapment efficacy might be due to the extreme drug wastage and carrier that necessitated the drug moieties at the targeted site. Hence, the experimental results reveal that enhanced drug loading into the polymer allows them to diffuse out of the matrix without any significant biological effort.

In vitro drug release studies

The *in vitro* drug release studies were performed by using dialysis diffusion bag method for 24 hr in phosphate buffer pH 7.4 at 37±0.5°C. As the polymeric concentration increases, the drugs release decrease, because a thick polymeric matrix prevents the drug entities to diffuse through the nanoparticles and makes their availability in the external compartment. The drug diffusion studies reveal that CTF1 showed maximum drug release 90.82% followed by CTF2 with 88.60% and CTF8 with least drug release of 72.59% (Table 3). The underlying theory is discussed in the earlier sections where the enormous increase in the polycaprolactone initiated the drug molecules to diffuse into the aqueous phase and decreased their availability for effective interaction with the polycaprolactone. In addition, the unfinished drug release is also due to the hydrophobic and crystalline nature of polycaprolactone which could be adjusted by preferring polymeric blends with Polylactic Acid (PLA) or Polylactic-co-Glycolic Acid (PLGA) or Polyethylene Glycol (PEG). However, the increased polycaprolactone concentration from CTF1 to CTF8 has increased the particle size of the nanoparticles and its drug content proportionally. Since the particle size of the drug particles is small it initiated the particles to release maximum druin due course of time.

Drug release kinetics

The drug diffusion studies were subjected to various kinetic models such as first order, Higuchi, and Korsemeyer-Peppas model (Table 3) to enumerate the mechanism of drug release form the nanoparticles. The drug release kinetics represents a first order release mechanism and the drug release is dependent on its concentration in the nanoparticles. The buffer in the receiver compartment penetrates into the donor compartment containing nanoparticles through diffusion and initiates the drug release. After certain duration of time, the difference in the drug concentrations between the donor and the receiver compartment enhances the drug release from the nanoparticles. In addition, the secondary factors such as porosity, rate of diffusion, time, and polymer degradation are the critical factors that influence the drug release from the dosage form. The exponential values in the Korsemeyer-Peppas model were between >0.5 and <1.0 which suggested a non-fickian drug release mechanism.

Particle size analysis

The particle size should increase proportionally with the increase in polyvinyl alcohol and polycaprolactone concentrations. Because the low polyvinyl alcohol concentrations are not able to completely shield the particles at the interface and initiates coagulation that results in increase in the particle size. Furthermore, as the concentration of the polyvinyl alcohol increase, the complete shielding of the particles at the interface occurs and results in a smaller particle size formation. An enormous increase in the polyvinyl alcohol concentrations has led to the formation of micelles which in turn enhanced the osmotic pressure of the formulation and resulted in particle

Table 2: The experimental outcomes of drug content, entrapment efficacy, particle size and zeta potential of clotrimazole nanoparticles. The results are expressed in terms of mean±0.5.

Formulation	Drug Content (%)	Entrapment Efficacy (%)	Particle Size (nm)	Zeta Potential (mV)
CTF1	92.43±0.08	67±0.08	80.24±0.03	-21.9
CTF2	93.19±0.03	72±0.06	89.13±0.05	-20.5
CTF3	90.28±0.07	74±0.03	93.23±0.02	-19.2
CTF4	93.27±0.05	79±0.07	98.25±0.07	-18.6
CTF5	92.28±0.08	85±0.02	109.24±0.04	-17.9
CTF6	90.17±0.02	81±0.03	125.62±0.05	-16.8
CTF7	91.24±0.06	79±0.04	134.26±0.07	-15.2
CTF8	90.02±0.03	69±0.02	142.18±0.06	-13.2

Table 3: Drug Release Kinetics from CTF1 to CTF8.

Formulation code	% CDR (at 24 hrs)	Zero order R^2	First order R^2	Higuchi's R^2	Korsemeyer Peppa's	
					n	R^2
CTF1	90.82	0.832	0.996	0.947	0.817	0.900
CTF2	88.60	0.860	0.996	0.948	0.705	0.910
CTF3	86.86	0.882	0.994	0.958	0.779	0.937
CTF4	83.94	0.831	0.984	0.943	0.872	0.972
CTF5	81.96	0.856	0.995	0.972	0.758	0.954
CTF6	78.88	0.843	0.995	0.943	0.797	0.925
CTF7	75.09	0.840	0.983	0.952	0.881	0.930
CTF8	72.59	0.895	0.991	0.953	0.737	0.949

aggregation. Further, a proportionate increase in the polyvinyl alcohol concentrations shall oppose the shear force implied during the sonification and might result in large sized particles. The increase in the polycaprolactone concentrations shall increase the viscosity of the organic phase and result in large sized particles. In addition, the sonification can significantly reduce the particle size and an increase in the volume of the organic phase and prevents the coagulation of particles. In the present study, we observed particle sizes ranged from 80.24±0.03 to 142.18±0.06 nm. Notably, the application of CTF1, comprising 100mg of polycaprolactone and 0.065 of polyvinyl alcohol, led to the production of smaller particles measuring 80.24±0.03 nm (Table 2).

Zeta potential

The investigative studies preferred polycaprolactone for encapsulating the drug molecules because it degrades slowly and does not creates an acidic environment that hiders the absorption of drug molecules. The nanoparticles generated a negative charge at its surface which might be due to the carbonyl group of the polycaprolactone at the surface of the nanoparticle. Interestingly, the nanoparticles with lower polyvinyl alcohol concentrations produced enhanced negative charge on the surface when compared to those fabricated with higher polyvinyl concentrations. At extreme polycaprolactone concentration, the concentration of polyvinyl alcohol at the interface decreased which resulted in deshielding effect and altered the zeta potential. Hence, it is not advised to use extreme polymer concentrations that may destabilize the product. The zeta potential measurements revealed a range from -21.9 mV to -13.2 mV, while for CTF1, the specific value was found to be -21.9 mV (Table 2). This observed variation in zeta potential could potentially be attributed to the partial adsorption of clotrimazole on the nanoparticle surface. This phenomenon likely played a significant role in maintaining the stability of the nanoparticles.

Microscopic studies

Scanning Electron Microscopy

In the current investigation we have preferred SEM because of its numerous advantages such as enhanced resolution and magnification, and its potentiality to analyze a wide range of materials. The average particle size of clotrimazole nanoparticles was found to be less than 50 nm, spherical, partially separated and no sign of particulate aggregation. The nanoparticles revealed a uniform size and shape which complied with the theoretical standards and could be recommended for commercialization (C, D, E F).

Transmission Electron Microscopy (TEM)

The TEM studies are preferred for capturing the high resolution images and considered as the most potential technique for analyzing the morphological characteristics of nano particles. The TEM uses a high electronic beam to encompass through the specimen to generate an image of high resolution. The TEM analysis is also used for analyzing the purity of sample through differentiation between the non-EVs and EVs of similar particles. The confirmation enables to differentiate the skewed results and predict the exact physical attributes of the nanoparticles. The TEM studies of CTF1 nanoparticles polymeric nanoparticles revealed spherical shape with 10-50 nm size . However, the TEM images also revealed the presence of some particle aggregates which might have broken down using ultra sonification process at optimized conditions prior to drying. In the absence of sonification and optimized drying conditions, the particles tend to agglomerate with potent adhesive attractions and difficult to segregate.

Atomic Force Microscopy (AFM)

Atomic force microscopy is the most preferred technique for the surface characterization of polymeric nanoparticles at nanometer resolution. The AFM images at contact mode represent the deposition of nanoparticles on mica in which represent the magnified images of particle surface area and represent the line-scan images of the nanoparticles. The AFM images for

CFT1 nanoparticles revealed spherical shape with 25±10 nm in diameter and 40±15nm height. The AFM images reveal nosy images corresponding to particle agglomerates while the small particles were clear. The images also revealed the presence of microcrystal structures which might be due to the variation in temperature and humidity on the mica plate and encouraged the crystal growth. The nanoparticles can be easily segregated from the micro crystals on the basis of size variation and evince a reservoir for the controlled delivery of drug molecules.

X-ray Diffraction Analysis

The theoretical interventions for the XRD pattern of polycaprolactone reveals the presence of two distinct diffractive peaks at 2θ=21.9° and 24.2° with basal spacing of 0.412 and 0.325nm correlating to (110) and (200) planes of orthorhombic crystal planes of polycaprolactone. A similar XRD pattern was notices in the CTF1 polymeric nanoparticles and a shift in the diffraction peak from 2θ=21.9° to 2θ=21.34° indicates an appreciable increase in the distance between the polymeric chains corresponding to crystalline plane. In a similar fashion, the standard XRD pattern for polyvinyl alcohol points a diffractive peak at 2θ=19.2° which renders the semi crystalline nature of polyvinyl alcohol. The XRD pattern of CTF1 nanoparticles disclose a minor shift in the diffraction peaks from the standard XRD patterns of polycaprolactone and polyvinyl alcohol which infers a negligible interaction between them.

Antifungal investigations

The antifungal investigation for Clotrimazole and its embedded nanoparticles on both non-resistant and resistant strains of *C. glabrata* and *C. albincans* is mentioned in Table 4 for reference. The experimental investigations specified that the MIC and IC_{50} values for Clotrimazole are 3 times greater in resistant strains of *C. glabrata* and *C. albincans*. Further, the results revealed an elevated Minimum Inhibitory Concentration (MIC) and half Maximum Inhibitory Concentration (IC_{50}) concentrations for Clotrimazole nanoparticles which represented a sustained drug release. The inherent antifungal activity of polymeric nanoparticles is due to their effective interaction with the cell membrane, their localization and enhanced ROS production that lead to intracellular impairment for both resistant and non-resistant species. Furthermore, the inhibition kinetics explored the potentiality of clotrimazole polymeric nanoparticles in furnishing antifungal activity. The statistical results reveal the MIC of *C. glabrata* and *C. albincans* were found to be 6.4±0.3 and 7.8±0.5 whereas the same for $CLTF1NP_S$ were found to be 25.3±0.4 and 23.2±0.3 (Table 4) which revealed that the nanoparticles were nearly four times effective in producing the antifungal effect. The IC_{50} values for *C. glabrata* and *C. albincans* were found to be 88.2±2.2 and 113.2±1.3 while the same for polymeric nanoparticles were found to be 273.3±2.8 and 362.2±0.4 which revealed that the polymeric nanoparticles were effective in eradicating the various fungal infections. The antifungal investigations on the resistant cells of *C. glabrata* and *C. albincans* specified that the potency of nanocomposites in eliciting the antifungal activity. The nanoparticles specified the MIC of 26.4±0.7 with IC_{50} values of 189.2±1.7 for resistant cells of *C. glabrata* and for *C. albincans*, the MIC values were found to be 26.3±0.6 and the IC_{50} values were found to be198.4±1.5 respectively. The statistical data specified that the clotrimazole embedded polymeric nano composites were effective in combating potent fungal infections and could be encapsulated with various antifungal agents to produce a desired pharmacodynamic effect.

ROS Production

The ROS production in the fungal species is due to the oxygen metabolism and the clotrimazole reveals a negligible level of ROS and these concentrations declined when compared to the resistance cells. The antifungal species treated with naked polymeric nanoparticles revealed a marked increase in the ROS production in both the resistant and non resistance cells. However, a significant increase in the ROS production was observed upon treatment with CFT1 nanoparticles and the results inferred that the nanoparticles had not differentiated the resistant cells. The ROS accumulation is principally due to the cell death involved in the antifungal activity and the experimental investigations enumerated that the effectiveness of the nanoparticles might be due to the breakdown of the in cell mechanism in combating against the clotrimazole.

Table 4: MIC and IC_{50} values of *C. glabrata* and *C. albincans* for CTF1 nanoparticles.

Species	Clotrimazole		CTF1NPS	
	MIC	IC_{50}	MIC	IC_{50}
C. glabrata	6.4±0.3	88.2±2.2	25.3±0.4	273.3±2.8
C. albincans	7.8±0.5	113.2±1.3	23.2±0.3	362.2±0.4
C. glabrata (Resistant cells)	22.6±0.5	178.2±1.2	26.4±0.7	189.2±1.7
C. albincans (Resistant cells)	20.4±0.4	187.2±3.1	26.3±0.6	198.4±1.5

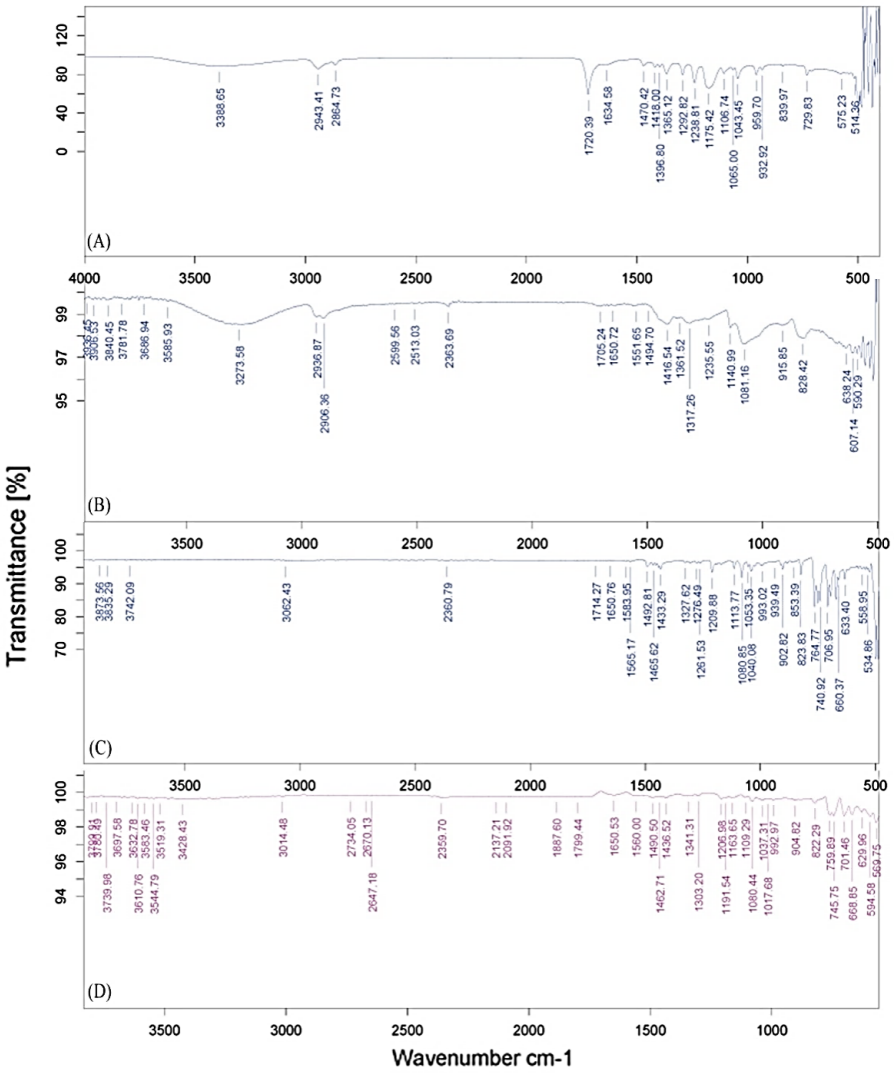

Figure 1: ATR Studies for (A) Polycaprolactone (B) Polycaprolactone (C) Clotrimazole (D) Combination of clotrimazole, polycaprolactone, and polyvinyl alcohol.

CONCLUSION

The research undertaken involved the meticulous fabrication and comprehensive analysis of clotrimazole-encapsulated polymeric nanoparticles, utilizing a range of concentrations of polycaprolactone and polyvinyl alcohol. The analysis of the nanoparticles produced pleasing results, showing a particle size range of 80.24±0.03 to 142.18±0.06 nm, and a significant variation in surface charge from 21.9 mV to -13.2 mV. Additionally, the FTIR and ATR studies confirmed the presence of important functional groups and the purity of the nanoparticles. The SEM, TEM, and AFM investigations provided detailed insights into the shape of the nanoparticles, demonstrating their spherical form with minimal clumping. Moreover, the detailed analysis revealed that the nanoparticles have an average diameter of 25±10 nm and a height measurement of 40±15 nm, allowing for a comprehensive understanding of their physical characteristics. This data indicates that the formulations possess a significantly enhanced surface area, which could potentially enable them to effectively penetrate cellular membranes and undergo internalization and lysis within the cells. Additionally, we carried out X-ray Diffraction (XRD) analyses, which confirmed the crystalline structure of the nanoparticles. Moreover, our antifungal investigations revealed interesting results, with the Minimum Inhibitory Concentration (MIC) values being measured at 25.3±0.4 and 23.2±0.3, and the half Maximal Inhibitory Concentration (IC_{50}) values being recorded at 273.3±2.8 and 362.2±0.4, respectively. The results show that the formulation is effective, especially in fighting against resistant strains of *C. glabrata* and *C. albicans*. The formulation's impressive antifungal activity indicates its potential for being marketed, especially in addressing various pathogenic fungi.

ACKNOWLEDGEMENT

The authors express their sincere gratitude to Annamacharya College of Pharmacy for the valuable facilities and support provided during their research.

ABBREVIATIONS

ATR: Attenuated total reflectance; **FTIR:** Fourier transform infrared spectroscopy; **XRD:** X-ray diffraction; **AFM:** Atomic force microscopy; **TEM:** Transmission electron microscopy; **CTF:** clotrimazole formulation; **ICDD:** International center of diffraction data; **MTCC:** Microbial type culture collection and gene bank; **MIC:** Minimum inhibitory concentration; **IC_{50}:** Half-maximal inhibitory concentration; **PEG:** Polyethylene glycol; **nm:** Nanometer; **mV:** Millivolts; **SD:** Standard deviation; **PLA:** Polylactic acid; **PLGA:** Polylactic-co-glycolic acid; **NPs:** Nanoparticles; **ROS:** Reactive oxygen species.

CONFLICT OF INTEREST

The authors declare that there is no conflict of interest.

SUMMARY

The study aimed to create and assess polymeric nanoparticles containing clotrimazole, using different concentrations of polycaprolactone and polyvinyl alcohol. The nanoparticles had a size range of 80.24±0.03 to 142.18±0.06 nm and a zeta potential range of -21.9 mV to -13.2 mV. Examination of their shape and aggregation revealed that they were mostly spherical with minimal clumping, and had an average diameter of 25±10 nm. Tests for antifungal properties showed MIC values of 25.3±0.4 and 23.2±0.3, indicating potential effectiveness against drug-resistant fungal strains.

REFERENCES

1. Shang L, Nienhaus K, Nienhaus GU. Engineered nanoparticles interacting with cells: size matters. J Nanobiotechnol 2014; 12: 5. https://doi.org/10.1186/1477-3155-12-5.
2. Rosales C, Uribe-Querol E. Phagocytosis: A Fundamental Process in Immunity. BioMed Research International 2017; 2017: 1–18. https://doi.org/10.1155/2017/9042851.
3. Pinto Reis C, Neufeld RJ, Ribeiro, AJ, Veiga F. Nanoencapsulation I. Methods for preparation of drug-loaded polymeric nanoparticles. Nanomedicine: Nanotechnology, Biology and Medicine 2006; 2: 8–21. https://doi.org/10.1016/j.nano.2005.12.003.
4. Rao JP, Geckeler KE. Polymer nanoparticles: Preparation techniques and size-control parameters. Progress in Polymer Science 2011; 36: 887–913. https://doi.org/10.1016/j.progpolymsci.2011.01.001.
5. Carrillo De Hert S, Rodgers TL. Continuous, recycle and batch emulsification kinetics using a high-shear mixer. Chemical Engineering Science 2017; 167: 265–77. https://doi.org/10.1016/j.ces.2017.04.020.
6. Božič M, Elschner T, Tkaučič D, Bračič M, Hribernik S, Stana Kleinschek K, *et al.* Effect of different surface active polysaccharide derivatives on the formation of ethyl cellulose particles by the emulsion-solvent evaporation method. Cellulose 2018; 25: 6901–22. https://doi.org/10.1007/s10570-018-2062-2.
7. Higazy IM, Mahmoud AA, Ghorab MM, Ammar HO. Development and evaluation of polyvinyl alcohol stabilized polylactide-co-caprolactone-based nanoparticles for brain delivery. Journal of Drug Delivery Science and Technology 2021; 61: 102274. https://doi.org/10.1016/j.jddst.2020.102274.
8. Afzal A, Jalalah M, Noor A, Khaliq Z, Qadir MB, Masood R, *et al.* Development and Characterization of Drug Loaded PVA/PCL Fibres for Wound Dressing Applications. Polymers 2023; 15: 1355. https://doi.org/10.3390/polym15061355.
9. Ekinci M, Yeğen G, Aksu B, İlem-Özdemir D. Preparation and Evaluation of Poly(lactic acid)/Poly(vinyl alcohol) Nanoparticles Using the Quality by Design Approach. ACS Omega 2022; 7: 33793–807. https://doi.org/10.1021/acsomega.2c02141.
10. Ahn K, Park K, Sadeghi K, Seo J. New Surface Modification of Hydrophilic Polyvinyl Alcohol via Predrying and Electrospinning of Hydrophobic Polycaprolactone Nanofibers. Foods 2024; 13: 1385. https://doi.org/10.3390/foods13091385.
11. Yin J-J, Burgess C, Shu L, Shumyak SP, Raymond N, Xu L, *et al.* Estrogen anchored nanomicelles for combinational drug delivery with enhanced therapeutic efficacy: a proteomics guided investigation for multifunctional nanotherapeutics. J Drug Delivery Ther 2018; 8: 41–53. Https://doi.org/10.22270/jddt.v8i2.1662.
12. Mahmoud MH, El-Gogary RI, Soliman ME, Kamel AO. Novel green-based polyglycerol polymeric nanoparticles loaded with ferulic acid: A promising approach for hepatoprotection. International Journal of Biological Macromolecules 2024; 264: 130698. https://doi.org/10.1016/j.ijbiomac.2024.130698.
13. Aljabbari A, Lokras AG, Kirkensgaard JJK, Rades T, Franzyk H, Thakur A, *et al.* Elucidating the nanostructure of small interfering RNA-loaded lipidoid-polymer hybrid nanoparticles. Journal of Colloid and Interface Science 2023; 633: 907–22. https://doi.org/10.1016/j.jcis.2022.11.141.
14. Tsilova SL, Schreiber BE, Lever R, Parhizkar M. Polymeric nanoparticles produced by electrohydrodynamic atomisation for the passive delivery of imatinib. European Journal of Pharmaceutics and Biopharmaceutics 2024; 202: 114412. https://doi.org/10.1016/j.ejpb.2024.114412.
15. Hnamte M, Pulikkal AK. Biocompatible polymeric nanoparticles as carriers for anticancer phytochemicals. European Polymer Journal 2024; 202: 112637. https://doi.org/10.1016/j.eurpolymj.2023.112637.
16. Imam F, Mukhopadhyay S, Kothiyal P, Alshehri S, Saad Alharbi K, Afzal M, *et al.* Formulation and characterization of polymeric nanoparticle of Rivastigmine for effective management of Alzheimer's disease. Saudi Pharmaceutical Journal 2024; 32: 102048. https://doi.org/10.1016/j.jsps.2024.102048.
17. Ghaemi A, Khanizadeh A, Pourmadadi M, Yazdian F, Rashedi H, Rahdar A, *et al.* Targeted Nano-Delivery of Flutamide with polymeric and lipid nanoparticles. European Polymer Journal 2024; 213: 113124. https://doi.org/10.1016/j.eurpolymj.2024.113124.
18. Bikiaris D, Karavelidis, Karavas, Giliopoulos, Papadimitriou. Evaluating the effects of crystallinity in new biocompatible polyester nanocarriers on drug release behavior. IJN 2011: 3021. https://doi.org/10.2147/IJN.S26016.
19. Gagliardi A, Giuliano E, Venkateswararao E, Fresta M, Bulotta S, Awasthi V, *et al.* Biodegradable Polymeric Nanoparticles for Drug Delivery to Solid Tumors. Front Pharmacol 2021; 12: 601626. https://doi.org/10.3389/fphar.2021.601626.
20. Thamilselvan G, David H, Sajeevan A, Rajaramon S, Solomon AP, Durai RD, *et al.* Polymer based dual drug delivery system for targeted treatment of fluoroquinolone resistant Staphylococcus aureus mediated infections. Sci Rep 2023; 13: 11373. https://doi.org/10.1038/s41598-023-38473-3.
21. Weng J, Tong HHY, Chow SF. In Vitro Release Study of the Polymeric Drug Nanoparticles: Development and Validation of a Novel Method. Pharmaceutics 2020; 12: 732. https://doi.org/10.3390/pharmaceutics12080732.
22. Mead H, Paraskevopoulou V, Smith N, Gibson R, Amerio-Cox M, Taylor-Vine G, *et al.* Developing a robust in vitro release method for a polymeric nanoparticle: Challenges and learnings. International Journal of Pharmaceutics 2023; 644: 123317. https://doi.org/10.1016/j.ijpharm.2023.123317.
23. Beach MA, Nayanathara U, Gao Y, Zhang C, Xiong Y, Wang Y, *et al.* Polymeric Nanoparticles for Drug Delivery. Chem Rev 2024; 124: 5505–616. https://doi.org/10.1021/acs.chemrev.3c00705.
24. Rathee J, Kaur A, Kanwar R, Kaushik D, Kumar R, Salunke DB, *et al.* Polymeric Nanoparticles as a Promising Drug Delivery Platform for the Efficacious Delivery of Toll-Like Receptor 7/8 Agonists and IDO-Inhibitor. Colloids and Surfaces A: Physicochemical and Engineering Aspects 2022; 632: 127764. https://doi.org/10.1016/j.colsurfa.2021.127764.
25. Pavaloiu R-D, Sha'at F, Hlevca C, Sha'at M, Savoiu G, Osman S. Evaluation of drug release kinetics from polymeric nanoparticles loaded with poorly water-soluble APIs. Ovidius University Annals of Chemistry 2021; 32: 132–6. https://doi.org/10.2478/auoc-2021-0020.
26. Zielińska A, Carreiró F, Oliveira AM, Neves A, Pires B, Venkatesh DN, *et al.* Polymeric Nanoparticles: Production, Characterization, Toxicology and Ecotoxicology. Molecules 2020; 25: 3731. https://doi.org/10.3390/molecules25163731.
27. Koniuch N, Ilett M, Collins SM, Hondow N, Brown A, Hughes L, *et al.* Structure of polymeric nanoparticles encapsulating a drug-pamoic acid ion pair by scanning transmission electron microscopy. Heliyon 2023; 9: e16959. https://doi.org/10.1016/j.heliyon.2023.e16959.
28. Fayed BE, Tawfik AF, Yassin AEB. Novel erythropoietin-loaded nanoparticles with prolonged in vivo response. Journal of Microencapsulation 2012; 29: 650–6. https://doi.org/10.3109/02652048.2012.680507.
29. Wilson BK, Prud'homme RK. Nanoparticle size distribution quantification from transmission electron microscopy (TEM) of ruthenium tetroxide stained polymeric nanoparticles. Journal of Colloid and Interface Science 2021; 604: 208–20. https://doi.org/10.1016/j.jcis.2021.04.081.
30. Malatesta M. Transmission Electron Microscopy as a Powerful Tool to Investigate the Interaction of Nanoparticles with Subcellular Structures. IJMS 2021; 22: 12789. https://doi.org/10.3390/ijms222312789.
31. Biran I, Houben L, Kossoy A, Rybtchinski B. Transmission Electron Microscopy Methodology to Analyze Polymer Structure with Submolecular Resolution. J Phys Chem C 2024; 128: 5988–95. https://doi.org/10.1021/acs.jpcc.3c06977.
32. Ponnamma D, Rouxel D, Thomas S. Spectroscopy-introducing the advantages and application areas in polymer nanocomposites. Spectroscopy of Polymer Nanocomposites, Elsevier; 2016, p. 1-14. https://doi.org/10.1016/B978-0-323-40183-8.00001-X.

33. Todaro B, Santi M. Characterization and Functionalization Approaches for the Study of Polymeric Nanoparticles: The State of the Art in Italian Research. Micro 2022; 3: 9-21. https://doi.org/10.3390/micro3010002.
34. Fayyadh SM, Ben Ahmed A. Nanocomposite-Supported Polymeric Composites Prepared with Different Deposition Bases: Characterization and Application in X-ray Shielding. Physics 2024; 6: 334-55. https://doi.org/10.3390/physics6010022.
35. Joshi J, Homburg SV, Ehrmann A. Atomic Force Microscopy (AFM) on Biopolymers and Hydrogels for Biotechnological Applications-Possibilities and Limits. Polymers 2022; 14: 1267. https://doi.org/10.3390/polym14061267.
36. Montasser I, Fessi H, Coleman AW. Atomic force microscopy imaging of novel type of polymeric colloidal nanostructures. European Journal of Pharmaceutics and Biopharmaceutics 2002; 54: 281-4. https://doi.org/10.1016/S0939-6411(02)00087-5.
37. Wang Y, Chen S, Hu A. Construction of Polyarylenes with Various Structural Features via Bergman Cyclization Polymerization. Top Curr Chem (Z) 2017; 375: 60. https://doi.org/10.1007/s41061-017-0145-4.
38. Ntow-Boahene W, Cook D, Good L. Antifungal Polymeric Materials and Nanocomposites. Front Bioeng Biotechnol 2021; 9: 780328. https://doi.org/10.3389/fbioe.2021.780328.
39. Abo El-Ela FI, Hassan WH, Amer AM, El-Dek SI. Antifungal Activity of Chitosan Polymeric Nanoparticles and Correlation with Their pH Against Mucor circinelloides Causing Mucormycosis, Along with *Penicillium notatum* and Aspergillus Species. Curr Microbiol 2024; 81: 47. https://doi.org/10.1007/s00284-023-03555-y.
40. Saleh N, Elshaer S, Girgis G. Biodegradable Polymers-based Nanoparticles to Enhance the Antifungal Efficacy of Fluconazole against *Candida albicans*. CPB 2022; 23: 749-57. https://doi.org/10.2174/1389201022666210708105142.
41. Alhowyan AA, Altamimi MA, Kalam MA, Khan AA, Badran M, Binkhathlan Z, *et al.* Antifungal efficacy of Itraconazole loaded PLGA-nanoparticles stabilized by vitamin-E TPGS: *In vitro* and *ex vivo* studies. Journal of Microbiological Methods 2019; 161: 87-95. https://doi.org/10.1016/j.mimet.2019.01.020.

Cite this article: Viswanath V, Krishna PVM, Babu VL, Lakkamma TAM. Formulation and Characterization of Clotrimazole Loaded Polymeric Nanoparticles Fabricated by Single Emulsion Evaporation Technique. Indian J of Pharmaceutical Education and Research. 2026;60(1s):s83-s92.